Influence of relative humidity on the photocatalytic oxidation (PCO) of toluene by TiO$_2$ loaded on activated carbon fibers: PCO rate and intermediates accumulation

Ting Guo, Zhipeng Bai *, Can Wu, Tan Zhu

State Environmental Protection Key Laboratory of Urban Ambient Air Particulate Matter Pollution Prevention and Control, College of Environmental Science and Engineering, Nankai University, Tianjin 300071, PR China

Abstract

Photocatalytic oxidation (PCO) tests were carried out for toluene adsorbed on the activated carbon fibers (ACFs)-supported TiO$_2$ photocatalyst in an environmental condition controlled chamber. TiO$_2$/ACF catalyst was made and characterized by N$_2$ adsorption isotherm for pore structure and scanning electron microscopy (SEM) for morphology, respectively. Through exploring the remnant of toluene and the accumulation of intermediates on the TiO$_2$/ACF catalyst including species, amount and their change processes under different relative humidity (RH), this study aimed to explore the influence of RH on the PCO of toluene and the roles of water vapor in the PCO process: PCO reaction paths and the accumulation of intermediates on the TiO$_2$/ACF catalyst. Results showed that (1) with the increase of RH in the chamber (15%, 30%, 45% and 60%) the PCO conversion rate of toluene was positive correlated and no catalyst deactivation was observed under all RH levels; (2) during the gas–solid PCO process of toluene, byproducts of aromatic ring oxidation including 2-methyl, p-benzoquinone and $o(m, p)$-cresol were observed on the TiO$_2$/ACF catalyst which had not been reported, together with the intermediates of side chain oxidation including benzyl alcohol, benzaldehyde and benzoic acid which had been reported; (3) although benzaldehyde was the primary intermediate under all RH level, amounts of the byproducts of aromatic ring oxidation were increased with the increase of RH; and (4) elevated RH increased the accumulation of benzyl alcohol but assuredly decreased the accumulation of benzaldehyde. These results suggested that (1) RH affects both the PCO rate and the PCO reaction path of toluene; (2) although methyl group oxidation is the major path, aromatic ring oxidation, which is not the expected path for the PCO of toluene, is enhanced when the RH increases; (3) apart from the role of hydroxyl radical ($^\bullet$OH) produced from water by TiO$_2$, water molecule also directly takes part in the PCO process. A hypothesis has been suggested: transition species comprised of benzaldehyde, hydroxyl and water molecule exists in the PCO conversion process from benzaldehyde to benzoic acid, though the hypothesis has not been confirmed.
© 2007 Elsevier B.V. All rights reserved.

Keywords: Photocatalytic oxidation; Intermediates; Relative humidity (RH); TiO$_2$/ACF; Toluene

1. Introduction

Volatile organic compounds (VOCs) are one group of the main pollutants in indoor air released from many kinds of sources and contribute negatively to human health. Despite the success of adsorption as a means to remove VOCs in indoor air, it does not actually destroy the pollutants but merely remove them for recycling elsewhere in the biosphere; moreover, saturation adsorption is another troublesome problem existing in the adsorption technique. Heterogeneous photocatalytic oxidation (PCO) [1,2] has been proposed as an advanced oxidation technique for mineralizing various environmental organic pollutants, especially for air decontamination. However, there are still issues unanswered in the application of the PCO technique. Some of these issues are (1) lower PCO rate than expected; (2) environmental toxicity and behaviors of intermediates; and (3) catalyst deactivation. Environmental relative humidity (RH) plays an important role on the gas–solid PCO process of VOCs. A large number of studies related to RH have been devoted to this field in the last two decades to address these issues mentioned above. The work presented here also addresses this topic.

* Corresponding author.
E-mail address: zbai@nankai.edu.cn (Z. Bai).

1.1. Relative humidity versus PCO rate

There are usually two kinds of rate definition used in PCO research. One is PCO conversion rate which equals the conversion amount of reactant per minute; the other is PCO mineralization rate which equals the yield of inorganic products (CO_2 is a common index) per minute.

Environmental RH significantly affects the rate of the gas–solid PCO and there still exist a lot of arguments concerning the effect [3–12]. Ibusuki and Takeuchi [7] studied the gas–solid PCO of toluene in a batch reactor with 10 min residence time and reported that no reaction products or decrease of toluene concentration was observed in a toluene–dry air system; in sharp contrast, CO_2 concentration in effluent stream after the PCO reaction was positively correlated with the RH levels over the range of 0–60%. Ameen and Raupp [6] reported supporting results: when RH was less than or equal to 70%, the PCO conversion rate increased with the increasing RH levels; high RH (above 80%) led to steady PCO conversion rate. Similarly, other researchers found that the PCO conversion rate had a peak value with increasing RH, which meant that trace water was necessary to maintain catalyst activity for extended periods of time, but high water level inhibited the PCO process [3,10–12]. Park et al. [8] claimed that the presence of water reduced the PCO conversion/degradation rate because water enhanced the efficiency of electron–hole recombination. Phillips and Raupp [9] proposed that the competitive adsorption of water and organic compounds on TiO_2 surface might cause a loss in PCO conversion rate at high RH level.

1.2. Relative humidity versus intermediates

The characterization of intermediates involved in the photocatalytic degradation of VOCs is important to avoid unwanted conversion of VOCs into more hazardous compounds. Recent research confirmed that during the gas–solid PCO of aromatics, no significant gas-phase intermediates were observed, but recalcitrant, strongly bound and partially oxidized reaction intermediates accumulated on the photocatalyst surface [3–8,13–18]. However, there are only a few gas–solid PCO studies on the relationship between RH and the distribution of intermediates [19]. Fujihira et al. [20,21] conducted studies from the liquid–solid PCO system and found the formation of the intermediates of cresols, benzyl alcohol, and benzaldehyde during the PCO of toluene in aqueous solution with pumped air bubble entering [20]; but only benzaldehyde was observed during the PCO of pure liquid toluene [21].

Accumulated amount of intermediate is also an important factor for the PCO process. In gas–solid PCO, the real photocatalytic active sites are on the surface of TiO_2. Since intermediates begin to accumulate on the active sites, it will decrease the availability of active sites and cause a decline in the degradation of toluene. Ameen and Raupp [6] found that the TiO_2 surface was covered by the reactant and aromatic partial oxidation intermediates, and the accumulated inter-

mediates contents were significantly higher in the condition of lower RH level through examining the PCO of *o*-xylene in a powder-layer reactor. Mendez-Roman and Cardona-Martinez [5] reported supporting observation that water vapor improved the catalyst regeneration processes due to its importance in the elimination of intermediate products which accumulated on the catalysts.

In summary, RH strongly affects the PCO effect/efficiency. Although various studies reported that intermediates accumulated on the surface of the photocatalyst, there are very limited studies published on the accumulated amount or the accumulation processes of these intermediates under different RH. Thus further studies should be helpful in the exploration of the PCO process, especially in revealing the reason of catalyst deactivation.

Toluene is a major indoor air pollutant and various studies have tested the potentiality in the use of gas-phase PCO of toluene for air decontamination [6–12]. In this paper, the PCO of toluene was studied using nano-TiO_2 immobilized on activated carbon fibers (ACFs). ACFs, a new formulation of activated carbon with high BET surface area and uniform micropore structure, were used to support nano-TiO_2 particles, adsorb toluene, and retain all intermediates during the PCO process. Toluene was adsorbed on the TiO_2/ACF catalyst in sample vial firstly, and then adsorbed toluene was photocatalytic degraded in an environmental condition controlled chamber. Elimination of toluene and accumulation of the intermediates under different RH were studied in order to explore the influence of RH on the PCO of toluene and the role of water vapor in the PCO process.

2. Experimental

2.1. Reagents

All reagents (toluene, benzyl alcohol, benzaldehyde, benzoic acid, 2-methyl, *p*-benzoquinone, *o*(*m*, *p*)-cresol and carbon disulfide) were of chromatogram purity grade (Guangfu Reagent Corporation, China). Water used for solution and experimental preparations was ultra-pure (18.2 MΩ cm resistivity; <10 ppb TOC) from Milli-Q plus (Millipore, USA).

2.2. TiO$_2$/ACF catalyst preparation

Nano-TiO_2 (Degussa P-25: surface area 50 m^2/g, nonporous, about 80% anatase) was used as a photocatalyst without any pretreatment. ACFs (Nantong Senyou Carbon Fibers Corporation, China), in the form of felt, were produced from rayon precursor. ACFs were washed with ultra-pure water and dried at 105 °C before use.

Pieces of ACFs (10 mm × 12 mm × 1 mm) were put into nano-TiO_2 water suspension (2 wt.%), under ultrasonic treatment for 60 min. Then the pieces (TiO_2/ACF catalysts) were dried at 105 °C for 2 h. In all experiments, the amount of TiO_2 of 5.2 mg ± 5% loaded on one piece of ACFs was determined by the difference of weight before and after the coating procedure.

2.3. Experimental setup

Adsorption was conducted in the EPA sample vials with PP Screw Seals (20 ml, ND 24, La-Pha-Pack, Germany). A stainless steel environmental condition controlled chamber (1 m × 1 m × 1 m, 1.5 mm thick, 1Ni18Cr9Ti) was employed for PCO degradation studies. Illumination was provided by a 15 W UV mercury lamp (Nanjing Jinling Lamp Corporation, China) which emits ultraviolet radiation with a primary wavelength at 254 nm. The UV lamp tube (length 50 cm) on a holder was vertically placed on the bottom of the chamber. A stainless steel circle plate (diameter 10 cm) with eight equiangular and spokewise stainless steel thread rods (diameter 2 mm, length 8 cm) was horizontally fixed in the middle of the lamp tube. Eight metal clamps were fixed on each rod by two hexagon thin nuts, respectively with a horizontal distance of 5 cm from the lamp tube surface. Surface of clamps was coated with Teflon film. Constant temperatures (T, $25 \pm 0.5\,°C$) and four RH levels (15%, 30%, 45% and 60%) in the chamber were achieved by a thermostatic and humidifier controller. Experimental setup is illustrated in Fig. 1.

2.4. Adsorption–degradation experiments

Adsorption procedure: nine TiO$_2$/ACF samples were put into nine sample vials, respectively, and then the vials were sealed. Each vial was carefully injected with 2.0 µl toluene by a syringe (10UL, Agilent Corp., USA), and then kept in darkness.

Degradation procedure: After 12 h, eight TiO$_2$/ACF samples were taken out from the vials, and fixed on the clamps, respectively. Lamp was turned on when the T and RH in the chamber reached the set condition. Six TiO$_2$/ACF samples were collected respectively at 30, 60, 90, 120, 150 and 180 min as the experimental samples. Two more TiO$_2$/ACF samples were collected at 90 and 180 min respectively, as the parallel samples. The ninth TiO$_2$/ACF sample, the control, was analyzed directly without exposure to UV light.

2.5. Instrumental analysis

2.5.1. Characterization of TiO$_2$/ACF

N$_2$ adsorption isotherm was measured at 77 K using a Micromeritics ASAP 2000 (Japan). The pore size distribution was calculated by the density functional theory (DFT) method [22]. The morphology of small TiO$_2$ particles on the ACFs was examined by a scanning electron microscope (SEM, Hitachi S-4500 Model, Japan).

2.5.2. GC–MS and GC–FID analysis

Accumulated intermediate organic products were extracted from the TiO$_2$/ACF samples by carbon disulfide (CS$_2$) under ultrasonication. Qualitative analysis of the filtrate was carried out by the use of an Agilent 6890 Gas Chromatograph equipped with a HP-5MS capillary column (length 30 m, i.d. 0.53 mm, film thickness 0.25 µm) and a HP 5975 mass analyzer detector.

Accumulated intermediate organic products and remaining reactant were extracted from each TiO$_2$/ACF sample by 2 ml carbon disulfide with 10 min ultrasonication. Quantitative analysis of the extraction was done by GC (Agilent 6890, Agilent Corp., USA) equipped with a HP-5MS capillary column and a FID detector.

2.6. QA and QC

2.6.1. Analytical quality of GC

Linearity of detector in response for all target organic compounds was evaluated using five-point calibrations covering the full range of concentration recorded in this study by direct injection of known amounts of toluene, benzyl alcohol, benzaldehyde, benzoic acid, 2 methyl, *p*-benzoquinone and *o*(*m*, *p*)-cresol dissolved in carbon disulfide. The correlation coefficient for all calibration curves exceeded 0.998.
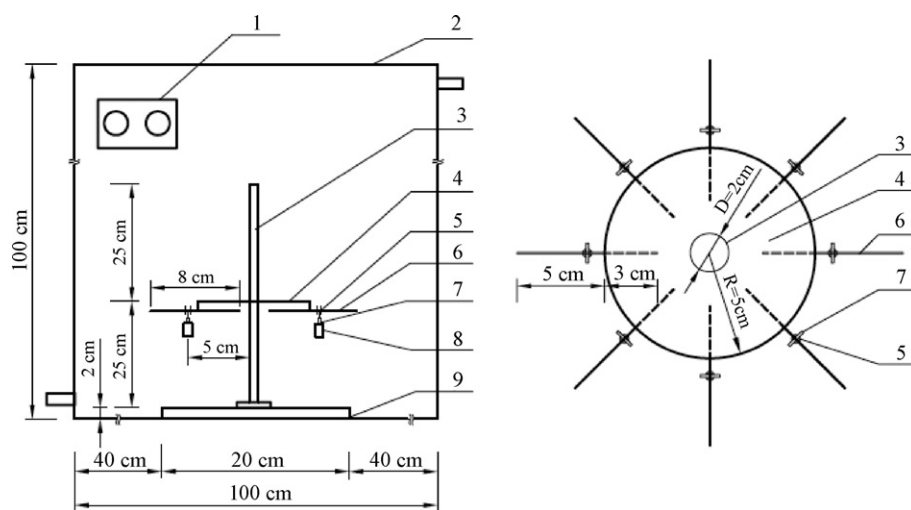

Fig. 1. A schematic diagram of the experimental setup. Left: side view of the experimental setup; right: top view of the stainless steel circle plate. (1) Thermo/humidity controller; (2) environmental condition controlled chamber; (3) UV lamp (254 nm); (4) stainless steel circle plate; (5) hexagon thin nut; (6) stainless steel thread rod; (7) clamp; (8) TiO$_2$/ACF catalyst; (9) lamp holder.

2.6.2. Recovery efficiency

Six TiO$_2$/ACF samples were put into six vials, respectively, and then vials were sealed. Each vial was injected with 0.2, 0.6, 1.2, 1.6, 2.2 and 2.6 μl toluene, respectively, and then they were kept in darkness. Twelve hours later, these samples were taken out, transferred to another vial, and analyzed to make the work curve. The correlation coefficient for the work curve was 0.993. The comparison of the work curve and the calibration curve revealed that the recovery efficiency of toluene was 100.2%. By the same method, the recovery efficiency of benzyl alcohol, benzaldehyde, 2-methyl, *p*-benzoquinone, and cresol was determined as 100.5%, 100.2%, 95.4%, and 98.7%, respectively.

2.6.3. Analytical precision

Five TiO$_2$/ACF parallel samples were analyzed using the method above (see Section 2.6.2) to check the analytical precision. And the relative standard deviations (R.S.D.) were less than 0.8% for all target compounds.

2.6.4. Blank material

Five pieces of TiO$_2$/ACF catalyst sealed in sample vials were analyzed to check any organic compound contamination in sample handling, transportation and storage. No target organic compounds were found in the blank material.

2.6.5. Control experiments

Two special absorption–degradation experiments were carried out at 60% RH level as control groups. One is using TiO$_2$/ACF with no illumination to check the diffusion loss of toluene during the dark procedure. The other is using original ACFs (no TiO$_2$ coated) with UV illumination to check any conversion of toluene and yields of intermediate organic compounds during the photooxidation procedure. No peak other than toluene was found through GC–FID analysis and no loss of toluene was found within the range of experimental error (2.0%).

2.6.6. Quality control

Sample vials were baked at 500 °C for 2 h in the muffle oven before use to assure minimal memory of the organic components. One control sample (see Section 2.4) was conducted for each experiment to check GC analytical quality.

3. Results

3.1. Pore size distribution and morphology of TiO$_2$/ACF

The scanning electron micrographs of original ACFs and TiO$_2$/ACF catalyst are shown in Fig. 2. Fine TiO$_2$ particles were coated on the substrate (ACFs), but were not uniformly distributed because of the fiber structure of ACFs. Nitrogen adsorption isotherms and pore size distributions for ACFs and TiO$_2$/ACF are shown in Fig. 3. The BET surface area of the original ACFs was 1215.4 m^2/g, and pores on ACFs were mainly micropores. For the TiO$_2$/ACF catalyst, BET surface area decreased to 999.6 m^2/g. From the pore size distribution
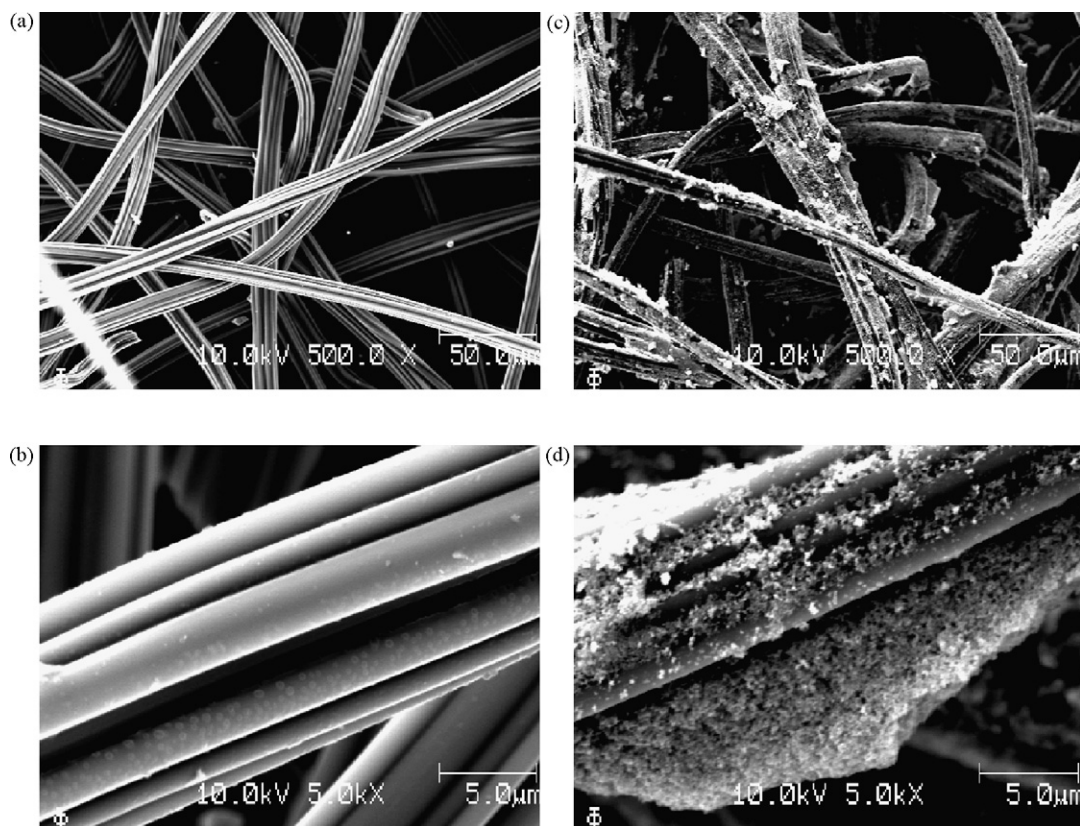

Fig. 2. Scanning electron micrographs of original ACFs (a and b) and TiO$_2$/ACF catalyst (c and d).
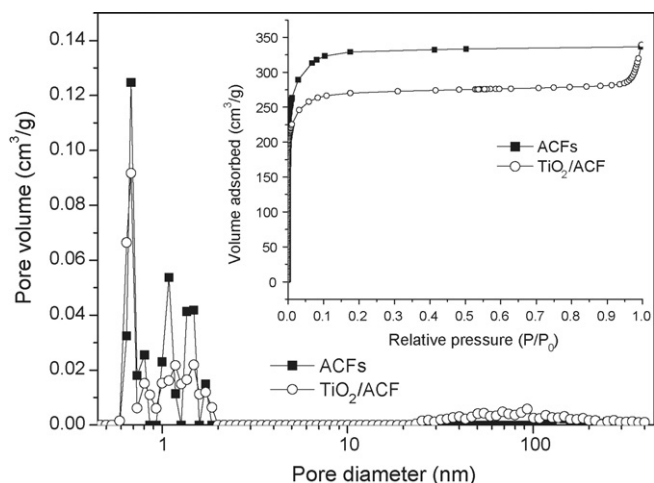
Fig. 3. Pore size distributions of original ACFs and TiO$_2$/ACF catalyst. Inset: N$_2$ adsorption isotherms of original ACFs and TiO$_2$/ACF catalyst.

Fig. 5. Accumulation amounts of five intermediate products on TiO$_2$/ACF catalysts after 180 min reaction at 15%, 30%, 45% and 60% RH levels.

curve, we can see that there was little change in the micropore size range, but a small portion of macropores were generated on TiO$_2$/ACF catalyst compared with the original ACFs due to TiO$_2$ particle agglomeration. These results indicated that the pore structure of ACFs remained the same. TiO$_2$ particles agglomerated only on the outside surface of ACFs, and the inside surface of ACFs was still exposed to the ambient.

3.2. Toluene removal

The conversion of toluene in 180 min under different RH is shown in Fig. 4. It showed that the oxidation conversion of toluene increased from 9.5% to 14.2% when the RH levels in the chamber increased from 15% to 60%. In the control experiments (see Section 2.6.5), no peak other than toluene was found through GC–FID analysis, and no loss of toluene was found. These results indicated that elevated RH increased the PCO conversion rate of toluene. The conversion rate of toluene
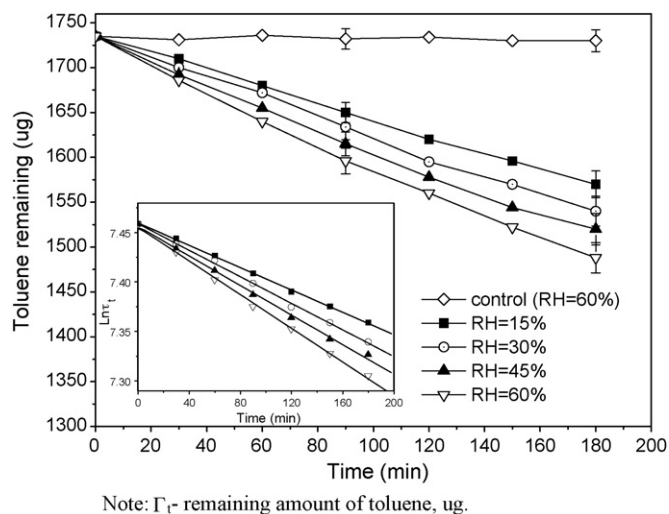
was not significantly diminished in 180 min, which indicated that no deactivation of catalyst occurred during the gas–solid PCO process in this study.

3.3. Intermediate organic products

Intermediate products accumulated on the TiO$_2$/ACF catalysts during the PCO of toluene were analyzed. Five intermediate products were detected as benzyl alcohol, benzaldehyde, benzoic acid, 2-methyl, *p*-benzoquinone and cresol by GC–MS. Amounts of these five accumulated intermediates were analyzed by GC–FID after 180 min reaction under four different RH. Results are shown in Fig. 5.

The accumulation of the intermediate products varied with the increase of RH. First, different levels of intermediate products were found accumulated on the TiO$_2$/ACF catalysts. Under all RH levels, benzaldehyde was the most abundant intermediate (about 74–89% by mass) and benzyl alcohol was

Fig. 4. Photocatalytic degradation behavior of toluene adsorbed on TiO$_2$/ACF catalyst at four RH levels of 15%, 30%, 45% and 60%. Inset: $\ln(\Gamma_t)$ vs. time.
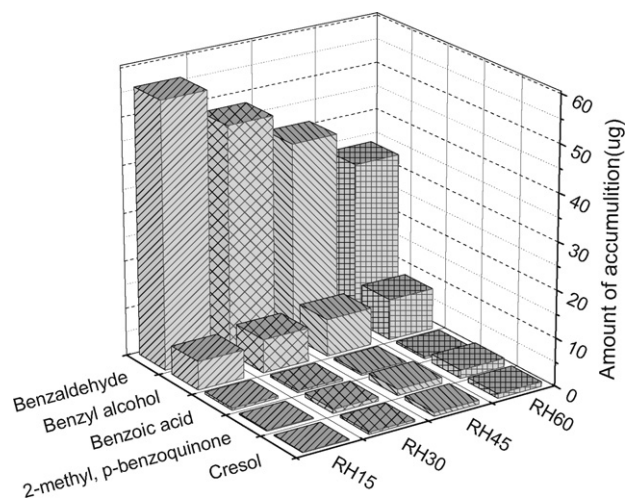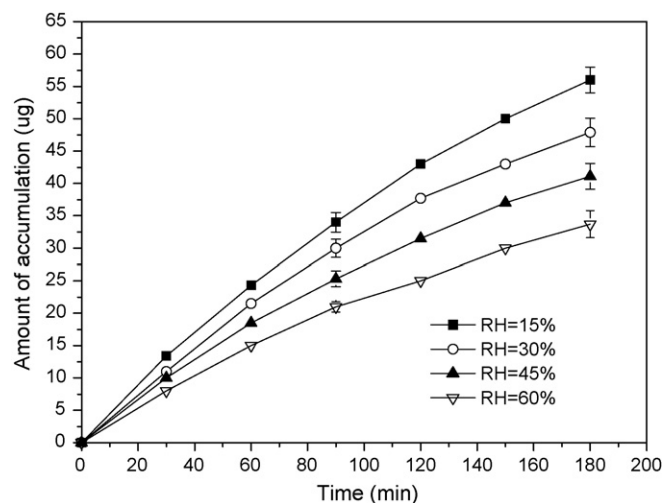
Note: Γ_t - remaining amount of toluene, ug.

Fig. 6. Amounts of benzaldehyde accumulated on TiO$_2$/ACF catalyst vs. time as a function of RH.

the secondary (about 9–19%). Benzoic acid (about 1%), 2-methyl, *p*-benzoquinone (about 1–3%) and cresol (about 1–2%) were trace intermediates. Secondly, the changing trends of the accumulation amount of these intermediates were different. With the increase of the RH in the chamber, the accumulation amount differed for five intermediates: benzaldehyde decreased a lot; benzoic acid increased a little; benzyl alcohol, 2-methyl, *p*-benzoquinone and cresol increased a lot.

To explore the detailed reason for the influence of the RH in the chamber, the accumulation processes of benzaldehyde and benzyl alcohol were studied and the results are shown in Figs. 6 and 7, respectively. It can easily be found that the accumulation behaviors of benzaldehyde and benzyl alcohol were opposite. The accumulation rate of benzaldehyde on the catalyst decreased significantly with the increase of RH, however, the accumulation rate of benzyl alcohol increased strongly.

Fig. 7. Amounts of benzyl alcohol accumulated on TiO_2/ACF catalysts vs. time as a function of RH.

4. Discussion

4.1. Reaction path

There are two kinds of hydrogen atom in a toluene molecule: one is in the methyl group, the other is in the aromatic ring. It is accepted that the oxidation of toluene takes place on the methyl group and proceeds in the following reaction chain: toluene → benzyl alcohol → benzaldehyde → benzoic acid → ⋯ → carbon dioxide [16,17]. At the same time, the oxidation of toluene taking place on the aromatic ring as a minor path has been proposed in aqueous solution [20] without much certainty during the gas–solid PCO process [17]. A schematic of the possible degradation paths of toluene is shown:

- *Path I*: Side chain (methyl group) oxidation.
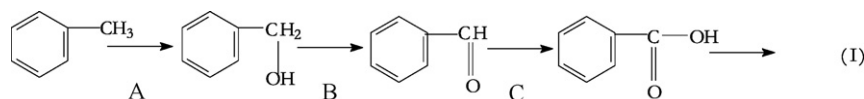
- *Path II*: Aromatic ring oxidation.
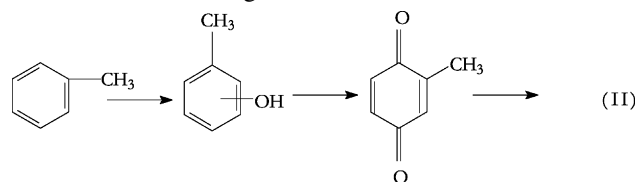
In this study, the formation of benzyl alcohol, benzaldehyde and benzoic acid that have been reported by other researchers [3,5,13,16,17] confirmed the occurrence of path I. At the same time, some intermediate products of the aromatic ring oxidation including 2-methyl, *p*-benzoquinone and cresol were also observed in the extraction of the TiO_2/ACF samples, which confirmed the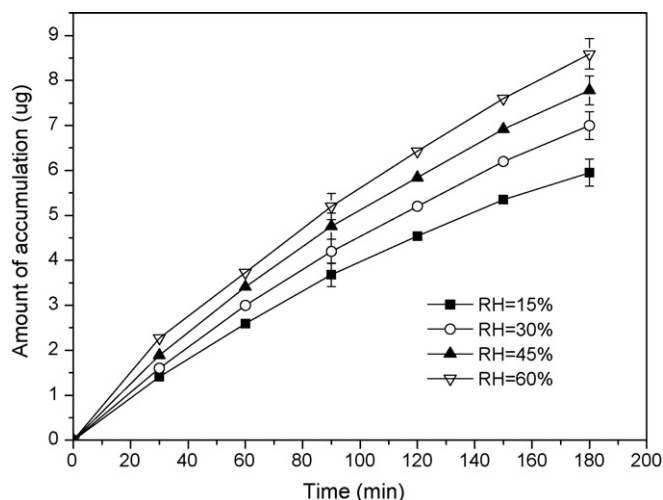 occurrence of path II. However, the intermediate products of the aromatic ring oxidation are usually more inhibitory and difficult to oxidize than those of the side chain oxidation. Larson and Falconer [17] reported that the adsorbed *m*-cresol was photocatalytically oxidized with difficulty by TiO_2 catalyst and the catalyst also turned black due to the polymerization of *m*-cresol to polyphenolic compounds. So, path II is not favored for the PCO of toluene.

Benzyl alcohol, benzaldehyde and benzoic acid were found in all experiments and benzaldehyde was also the most abundant intermediate under all RH. These results indicated that the methyl group oxidation is the main PCO reaction path of toluene. The aromatic ring oxidation is a minor PCO reaction path of toluene because only trace byproducts of this reaction path were observed. The accumulation amount of the intermediates of aromatic ring oxidation increased with the increase of RH. The distribution sketch map for the intermediate products of side chain oxidation and aromatic ring oxidation after 180 min reaction at 15%, 30%, 45% and 60% RH levels is shown in Fig. 8. It indicates that RH changed the PCO reaction process of toluene. The aromatic ring oxidation was enhanced when RH increased. Considering the environmental toxicity and PCO behaviors of these intermediates, more attention to the PCO of aromatic compounds under high water vapor level is justified.

4.2. Roles of water vapor

With the increase of RH, the intermediates of side chain oxidation displayed quite different accumulation behaviors on the TiO_2/ACF samples (Figs. 6 and 7). Elevation of RH in the chamber increased the accumulation of benzyl alcohol and significantly decreased the accumulation of benzaldehyde.

A competitive adsorption between water and organic compounds on catalyst surface had been proposed [9]. However, we can confirm that it is not the competitive adsorption between water and benzaldehyde that caused the reduction of benzaldehyde accumulation on the TiO_2/ACF photocatalyst when environmental RH was high. First, benzaldehyde is more strongly bound to TiO_2 than toluene, and there is no elimination of toluene by desorption even at 60% RH (control experiment). Secondly, TiO_2 was immobilized on ACFs, which has large adsorption capacity. So, the problem of competition for adsorption sites between water vapor and organic compounds can successfully be resolved.

In our experimental system, the conversion rate of toluene displayed as a first-order reaction and the increase of RH in the environmental chamber enhanced the PCO conversion rate of toluene, which indicated that the apparent reaction rate constant (k) of the conversion of toluene increased (Fig. 4). Hydroxyl radical arising from water by TiO_2 is often assumed to be the major active species to oxidize pollutants without selectivity for aqueous PCO process, however their role in gas-phase PCO is debated [13]. Under fixed illumination intensity, increase of RH in the environmental chamber presumably caused an enhancement of the concentration of OH radical, which could be responsible for the increase of the apparent k. Meanwhile, the increase of the apparent k also suggested that OH radical is the active species in gas–solid PCO system. According to the reaction dynamic principle, the increase of the apparent k of reactant should enhance the accumulation rate of the intermediates. In our experimental system, the accumulation rate of the intermediates increased with the increase of the RH except that of benzaldehyde. So, beside the role of the OH radical, water vapor must have played another role and significantly affect the dynamic behavior of benzaldehyde.

The photocatalytic oxidation from benzaldehyde to benzoic acid can be simply shown as reaction C1:

(C1)

(C2)
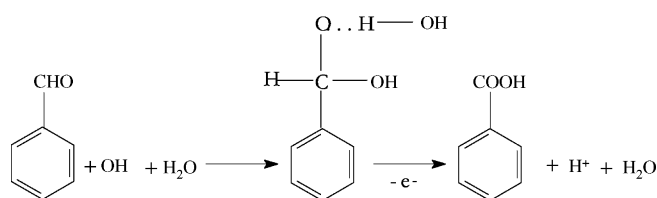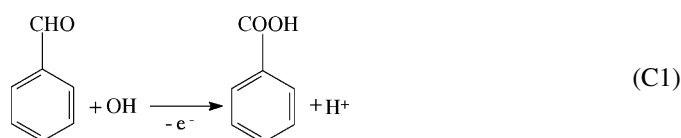
Based on the following two facts that (1) the radical of C_6H_5CO is unstable and (2) free radical substitution reaction is more difficult than free radical addition reaction for the oxidation of aromatic aldehyde to aromatic acid, we suggest a possible PCO mechanism from benzaldehyde to benzoic acid shown in reaction C2. Although no water exists in reaction C1, reaction C2 is consistent with our experimental data. Here, we suggest the
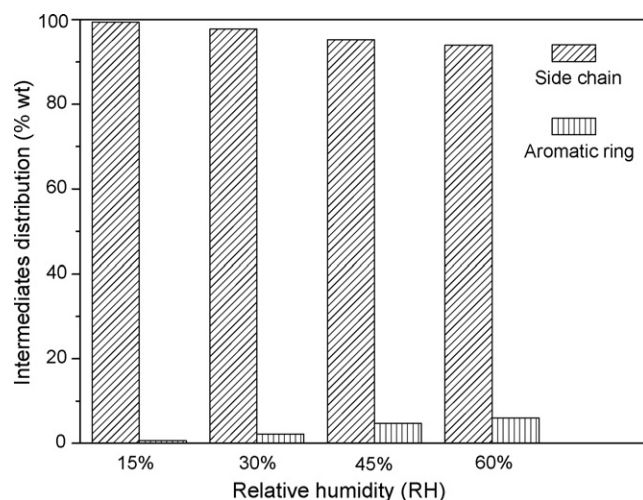

Fig. 8. Distribution sketch map for intermediate products of side chain oxidation and aromatic ring oxidation after 180 min reaction at 15%, 30%, 45% and 60% RH levels.

existence of a transition species comprised of benzaldehyde, hydroxyl, and water in the reaction process though it has not been confirmed yet. We believe that although OH radical is the real active species to oxidize benzaldehyde, water molecular also directly takes part in the PCO process from benzaldehyde to benzoic acid. The increase of the RH benefits the formation of the hydrated transition species, which enhances the conversion of benzaldehyde and causes the visible elimination of this intermediate compound. In conclusion, water vapor plays two kinds of roles during the PCO of toluene: one arises from the hydroxyl radical which acts as the active species to oxidize pollutants; the other arises from water molecular which improves the elimination of accumulated benzaldehyde.

4.3. Species for deactivation

Some researches suggested that it is the nonvolatile carboxylic acid or carboxylate that leads to the deactivation of catalyst [23]. These authors thought that carboxylic acids, usually nonvolatile and with strong bond with catalyst, would accumulate on the surface of photocatalysts and block the active sites on the photocatalysts. However, data from our experiments are inconsistent with this conclusion. If benzoic acid blocks the active sites on the photocatalysts and causes the decline of catalyst activity, a significant accumulation of benzoic acid in the experiment should be observed. However, only trace benzoic acid was observed during the PCO process.

Meanwhile, benzaldehyde was the most abundant compound among all intermediate products accumulated on the photocatalyst under all RH. It indicated that benzaldehyde is more difficult to oxidize than benzoic acid and the step from benzaldehyde to benzoic acid should be the slowest step during the PCO process of toluene. Although there was no deactivation in our experiments, we believe that it is benzaldehyde that should be responsible for the deactivation of photocatalyst in gas–solid system. Besides, due to their quite inert PCO behavior, the accumulated intermediates of aromatic ring oxidation will also be the species for the photocatalyst deactivation especially when the environmental RH is very high.

4.4. Merit of TiO₂/ACF

Deactivation of the photocatalyst has been regarded as a fatal disadvantage of the PCO technique in practice and it has involved the attention of many researchers aiming at the development of this new technique. When using the bare nano-TiO₂ as the photocatalyst, catalyst deactivation concomitantly exists in the gas–solid PCO process of aromatics, especially under low RH condition [3,6,7]. However, in our study, no catalyst deactivation was observed under any RH conditions. Nano-TiO₂ particles agglomerated only on the outside surface of ACFs, while the inside surface of ACFs was still exposed to the air (Fig. 2). The exposed ACFs served as the adsorption centers of pollutants, water and intermediates by physical or chemical process, allowing intermediate accumulated on the catalyst surface without hampering the interaction between pollutant and TiO₂, and reducing the competitive adsorption between pollutants and water [24–28]. So, we believe that lacking active sites is the reason for the deactivation of catalysts and the negative effect of water under high RH. TiO₂/ACF composite material, with large surface, is a good photocatalyst suitable for the abatement of catalyst deactivation problem.

5. Conclusions

(1) Increase of RH (15–60%) in the environmental chamber accelerated the PCO conversion rate of toluene and no deactivation of TiO₂/ACF catalyst was observed in all experiments.
(2) Our study confirmed that PCO conversion of toluene goes through two competitive paths, side chain oxidation and aromatic ring oxidation. RH in the environmental chamber affected the PCO reaction path. Aromatic ring oxidation was enhanced when RH increased, which is not favored considering the environmental toxicity and inert PCO behaviors of their intermediates. So, more attention to the PCO of aromatic compounds under high water vapor level is justified.
(3) Benzaldehyde was the most abundant compound among all intermediate products accumulated on the catalyst and it may be responsible for the deactivation of catalyst in the gas–solid PCO system.
(4) Water vapor plays two kinds of roles during the PCO of toluene: one arises from the hydroxyl radical which acts as the active species to oxidize pollutants; the other arises from water molecular which improves the elimination of accumulated benzaldehyde. A hypothesis was suggested: transition species comprised of benzaldehyde, hydroxyl, and water molecular exists in the PCO conversion process from benzaldehyde to benzoic acid, though the hypothesis has not been confirmed yet.
(5) TiO₂/ACF composite material with uniform micropore structure and large surface is a good photocatalyst suitable for the abatement of catalyst deactivation problem.

References

[1] A. Fujishima, T.N. Rao, D.A. Tryk, J. Photochem. Photobiol. C 1 (2000) 1–21.
[2] D.F. Ollis, C.R. Sci. Paris, Serie IIc, Chim./Chem. 3 (2000) 405–411.
[3] Y. Lou, D.F. Ollis, J. Catal. 163 (1996) 1–11.
[4] M.L. Sauer, M.A. Hale, D.F. Ollis, J. Photochem. Photobiol. A 88 (1995) 169–178.
[5] R. Mendez-Roman, N. Cardona-Martinez, Catal. Today 40 (1998) 353–365.
[6] M.M. Ameen, G.B. Raupp, J. Catal. 184 (1999) 112–122.
[7] T. Ibusuki, K. Takeuchi, Atmos. Environ. 20 (1986) 1711–1715.
[8] D.R. Park, J. Zhang, K. Ikeue, H. Yamashita, M. Anpo, J. Catal. 185 (1999) 114–119.
[9] L.A. Phillips, G.B. Raupp, J. Mol. Catal. 77 (1992) 297–311.
[10] J. Peral, D.F. Ollis, J. Catal. 136 (1992) 554–565.
[11] L.A. Dibble, G.B. Raupp, Catal. Lett. 4 (1990) 345–354.
[12] L.A. Dibble, G.B. Raupp, Environ. Sci. Technol. 26 (1992) 492–495.
[13] O. d'Hennezel, P. Pichat, D.F. Ollis, J. Photochem. Photobiol. A 118 (1998) 197–204.
[14] M. Lewandowski, D.F. Ollis, Appl. Catal. B: Environ. 43 (2003) 223–238.
[15] M. Lewandowski, D.F. Ollis, Appl. Catal. B: Environ. 43 (2003) 309–327.
[16] L. Cao, Z. Gao, S.L. Suib, T.N. Obee, S.O. Hay, J.D. Freihauty, J. Catal. 196 (2000) 253–261.
[17] S.A. Larson, J.L. Falconer, Catal. Lett. 44 (1997) 57–65.
[18] S. Sitkiewitz, A. Heller, N. J. Chem. 20 (1996) 223.
[19] E. Berman, J. Dong, in: Proceedings of the Third International Symposium on Chemical Oxidation Technology for the Nineties, Vanderbilt University, Nashville, TN, February 17–19, 1993.
[20] M. Fujihira, Y. Satoh, T. Osa, Nature 293 (1981) 206–207.
[21] M. Fujihira, Y. Satoh, T. Osa, J. Electroanal. Chem. 126 (1981) 277.
[22] J.P. Olivier, M.L. Occelli, J. Phys. Chem. B 105 (2001) 623–629.
[23] N.R. Blake, G.L. Griffin, J. Phys. Chem. 92 (1988) 5697–5701.
[24] J. Matosab, J. Lainteb, J.-M. Herrmann, J. Catal. 200 (2001) 10–20.
[25] C.H. Ao, S.C. Lee, J. Photochem. Photobiol. A 161 (2004) 131–140.
[26] C.H. Ao, S.C. Lee, Appl. Catal. B: Environ. 44 (2003) 191–205.
[27] J. Araña, J.M. Doña Rodríguez, C. Garriga i Cabo, O. González Díaz, J.A. Herrera Melián, J. Pérez Peña, Appl. Catal. B: Environ. 44 (2003) 153–160.
[28] J. Araña, J.M. Doña Rodríguez, C. Garriga i Cabo, O. González Díaz, J.A. Herrera Melián, J. Pérez Peña, Appl. Catal. B: Environ. 44 (2003) 161–172.